Journal Pre-proof

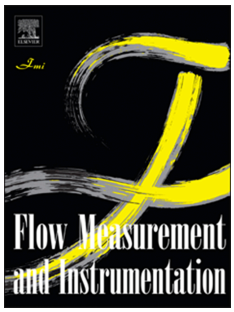

Experimental assessment on the performance of hot wire anemometry in and around a permeable medium by comparison with Particle Image Velocimetry

Nicolás Silin, Diego Cuscueta, Alejandro Clausse

PII: S0955-5986(20)30168-0

DOI: https://doi.org/10.1016/j.flowmeasinst.2020.101827

Reference: JFMI 101827

To appear in: *Flow Measurement and Instrumentation*

Received Date: 17 January 2020

Revised Date: 25 August 2020

Accepted Date: 1 September 2020

Please cite this article as: Nicolá. Silin, D. Cuscueta, A. Clausse, Experimental assessment on the performance of hot wire anemometry in and around a permeable medium by comparison with Particle Image Velocimetry, *Flow Measurement and Instrumentation* (2020), doi: https://doi.org/10.1016/j.flowmeasinst.2020.101827.

Experimental Assessment on the Performance of Hot Wire Anemometry in and around a Permeable Medium by comparison with Particle Image Velocimetry

Nicolás Silin[1], Diego Cuscueta[1] and Alejandro Clausse[2]

[1]Consejo Nacional de Investigaciones Científicas y Técnicas and Instituto Balseiro, Centro Atómico Bariloche, Av. Bustillo 9500, (8400) Bariloche, Argentina.

[2]Comisión Nacional de Energía Atómica, CONICET and Universidad Nacional del Centro, Pinto 399, (7000) Tandil, Argentina.

Abstract

The air flow through a test section partially obstructed by a permeable array of wires was measured simultaneously by Hot Wire Anemometry (HWA) and Particle Image Velocimetry. The objective of the study was the assessment of the suitability of HWA for the measurement of flow velocities amid and adjacent to groups of small obstacles. In the present case the obstacles are set in a regular array configuring a highly permeable structure. The probe was placed at three characteristic positions: in the free flow close to the wire array, inside the permeable medium, and at the interface between the permeable structure and the free flow. The measurements were performed with the hot wire operating under natural convection and mixed convection heat transfer, and operating the hot wire at different overheat ratios. Natural convection plumes extending over several permeable volume elements were detected when the hot wire was under natural convection, in some cases reaching velocities up to 60 mm/s downstream from the hot wire position. For low velocity flows, natural convection can be regarded as a flow velocity offset, which becomes negligible at local velocities higher than 0.03 m/s. For higher velocities, in the mixed convection regime, the intrusivity of the HWA probe becomes relevant. Furthermore, the flow in the test section used in the study presents a linear instability that produces velocity fluctuations. Availing ourselves of this phenomenon we verified the dynamic response of the HWA at the lowest velocity where the flow shows periodic fluctuations; for a local mean velocity of (0.131 ± 0.012) m/s the HWA showed a satisfactory dynamic response up to 20 Hz.

Keywords

HOT WIRE ANEMOMETRY, PERMEABLE MEDIUM, LOW SPEED, POROUS MEDIA, NATURAL CONVECTION, PARTICLE IMAGE VELOCIMETRY

Introduction

In the last years there has been a growing interest in compound flows that involve free flow regions and patches occupied by complex obstructions. These complex obstructions can be either natural — such as vegetation, hair or other naturally occurring element arrangements — or man-made — such as metal foams, tube banks, fins, pin arrays or other easily penetrable roughnesses (Gayev and Hunt, 2007). The interest in such flow systems comes from applications like plant physiology (Finnigan et al, 2009) and airfoil noise suppression (Bodling and Sharma, 2018; Clark et al, 2017). In particular complex obstructions can influence the stability of flows (Breugem et al, 2006; Silin et al,

2011; Ledda et al, 2018) and therefore can also be applied in passive turbulence control (Rosti et al, 2018). These flow systems are challenging, both numerically and experimentally, due to the broad range of spatial and temporal scales that are involved (Ghisalberti, 2009). The general experimental problem is that in these flows the fluid velocity spans over several orders of magnitude, being very low in the obstructed zones and comparatively high in the surrounding free flow regions.

An important difficulty to get information about the small scale flow structures inside permeable patches is the limitation or simply lack of optical access, which precludes or complicates the application of optical techniques such as Particle Image Velocimetry (PIV) or Laser Doppler Anemometry. In some limited cases the problem can be confronted using index matching strategies, but this is rather limited to specific test section materials and liquids (Harshani, 2017). An alternative method is Hot Wire Anemometry (HWA), which is a preferred technique in a number of situations, namely, boundary layers (Ikeya et al, 2017), when there is no optical access, where the velocity range spans several orders of magnitude (Ali et al, 2018), or where small but rapid fluctuations need to be identified (Ho and Asai, 2018). However, HWA does present various limitations, mainly because it is intrusive and difficult to calibrate in permeable media. A major challenge, for example, is applying HWA to measure laminar stability boundaries in flows involving complex obstructions, where the inner velocities become particularly low (Silin et al, 2011).

When addressing very low velocities, like those encountered within permeable media, a condition of mixed convection may be reached where the natural convection self-induced by the hot wire competes with the externally forced convection. In such case, the HWA response deviates from the King's law and, more importantly, depends on the relative orientation between the external forced flow, the buoyancy forces and the hot wire axis. This operating region was studied in depth for unobstructed flows and a concise review can be found in Bruun (1996). Typically, the influence of self-induced natural convection on HWA measurements becomes significant in air flows at speeds below 0.2 m/s and consequently requires a special calibration (Yue and Malmström, 1998; Özahi et al, 2010; Ligrani and Bradshaw, 1987). Downward slow flows are particularly complicated, for the heat transfer shows a minimum at a finite flow velocity depending on the Grashof number. This phenomenon leads to velocity determination ambiguities limiting the experimental range of HWA.

Christman and Podzimek (1981) studied an upward flow with the hot wire in horizontal position, i.e., the forced flow and the hot wire self-induced natural convection are both upward and normal to the wire axis. With this setup the HWA response is monotonous and can be calibrated to measure velocities in the mixed-convection heat-transfer region (Mahajan and Mahajan, 1980; Farsad et al, 2019). In turn, many HWA studies were directed to horizontal flows, which are very common in experiments carried out in wind tunnels. In such cases, forced and natural convection interact nonlinearly, which also results in a minimum heat transfer before the forced flow velocity reaches zero, limiting the valid range where measurements can be performed (Collis and Williams, 1959). In permeable media natural convection flow is determined by the balance between drag and buoyancy forces (Fand et al, 1986). Furthermore, an important aspect that should be taken into account when performing HWA measurements in complex obstructions is the increase of heat transfer in the immediacy of solid walls, which is relevant in boundary layers. To date, the general consensus is that the main cause of this phenomenon is conductive heat transfer from the hot wire to the wall (Ikeya et al, 2017). Therefore, this aspect cannot be neglected when probing the interior of permeable media with HWA (Zanoun et al, 2009).

Since in most cases HWA still remains the only alternative for local flow measurements inside or around sets of obstacles, it is important to perform comparative measurements of HWA by designing experiments where other techniques can be applied. This is the central objective of the present study, which aims to assess the application of HWA for the measurement of flow velocities amid and adjacent to a porous obstruction with high permeability. In particular we used a vertical upward air flow in a rectangular channel partially obstructed by an array of wires with a diameter of 0.25 mm. The regular array allows optical access among the obstacles, thus enabling the simultaneous measurement with HWA and PIV. We explore the performance of the hot wire anemometer in the natural convection and mixed convection regimes that correspond to measurement scenarios of no forced flow and low velocity forced flow respectively. Measurements are compared and analyzed regarding the position and operating heat power of the hot wire. We also perform a measurement in transitional flow regime to test the transient response capability of the HWA inserted in the wire array.

Method and Experimental Setup

Test section

The measurements were carried out in a straight square channel partially obstructed by a regular array of wires. In Figure 1 we present a scheme of the measurement section showing the different positions of the hot wire probe that were investigated in the present work. The local flow field in the plane normal to the hot wire was simultaneously measured by Particle Image Velocimetry (PIV); the illumination setup is also shown in the figure. The obstruction is made with copper winding wires. The wires have (0.257±0.005) mm external diameter and the varnish layer has approximately 15 μm providing a high quality surface finish. In a previous work (Clausse et al, 2019) the permeability of the wire array was estimated as κ = (1.7±0.1) mm^2, under the assumption of a homogenized permeable medium model with Darcy volumetric force. The free flow region has a width of (10.4±0.2) mm and the channel depth is 100 mm. A diagram of the experimental device is shown in Figure 2, also showing the illumination system and the camera position. Air is forced along the channel by a small DC fan and recirculated forming a closed circuit. Two honeycomb blocks are used as flow straighteners, one at the entrance of the test section and another at the exit. The test section is positioned vertically with the flow direction upward, in the same direction as the flow resulting from the natural convection plume produced by the hot wire. Christman and Podzimek (1981) performed HWA measurements at low air flows, studying the response depending on the direction of the working flow respect to gravity, they found that only by setting the forced flow vertically upward the response of the HWA is monotonous in the whole range. Based on this finding we consider this flow configuration to be the best candidate for low velocity measurements. It was verified that the temperature difference between the flow in the test section and the ambient air stayed within 0.5 °C for all measurement conditions, and that the temperature in the test section remained between 20.0 °C and 22.0 °C. Further detail on the experimental setup can be found in Clausse et al (2019).

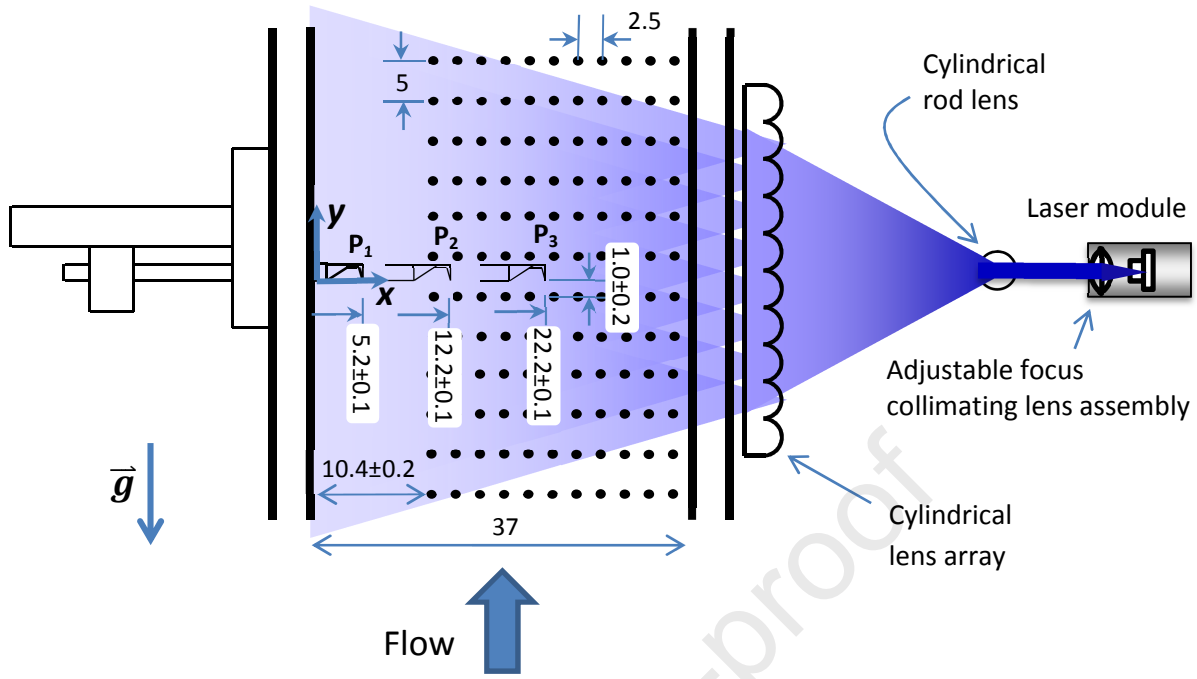

Figure 1. Diagram of the measurement section (all dimensions are in millimetres).

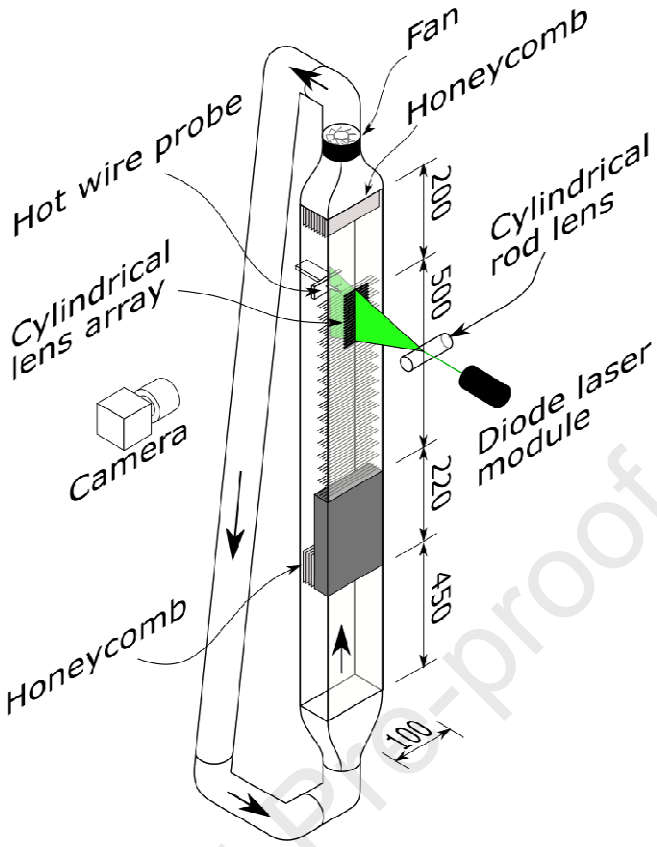

Figure 2 Diagram of the experimental device (all dimensions are in millimetres).

Particle Image Velocimetry

The flow seeding for PIV was olive oil droplets with a diameter of approximately 1 µm. PIV image pairs are captured by a BlackFly BFS-U3-13Y3M-C machine vision camera with a 35 mm lens at a framerate of 160 fps, thus obtaining 80 snapshots of the velocity field per second. The camera resolution is 1280 × 1024 pixel. Illumination pulses were produced by a Nichia NUBM44 laser diode module driven by the custom made electronic circuit described by Silin et al. (2017). The laser diode module includes a collimating glass lens assembly with adjustable focus in order to produce a collimated laser beam. The focus was adjusted in order to obtain a beam thickness of approximately 0.5 mm at P_2 (see Figure 1). The light sheet is generated from the laser beam using a cylindrical rod lens in combination with a cylindrical lens array, as shown in Figure 1. Figure 3 shows the photographs obtained with an illumination sheet generated by a cylindrical rod lens alone (left) and with the cylindrical lens array (right). The introduction of the cylindrical lens array solves the problem of the shadows behind the wires, which otherwise would result in an incomplete velocity field. The duration of the illumination pulse was set to 100 µs, resulting from a compromise between reaching the illumination energy necessary to capture low noise images of the particles and avoiding the particle images becoming streaks. A time lag of 1.5 ms was set between illumination pulses; which, for the present PIV processing parameters, imposes a velocity upper bound of approximately 0.6 m/s. The particle displacement between frames for velocities up to 0.1 m/s is 6.5 pixels,

approximately 0.15 mm. All PIV images were processed using the Robust Phase Correlation (Eckstein and Vlachos, 2009) implemented in the PRANA code (Drew et al., 2015). The processing was done in two passes; for the first pass we used a 128 × 64 pixel window, longer in the flow direction, and for the second pass a 32 × 32 pixel window. The measurement grid resolution was 16 × 16 pixel and the image resolution is 23.3 μm/pixel. A local outlier vector validation was applied to both steps. Averaged velocity fields were calculated from 80 snapshots for the cases where the flow was regarded as steady, and from 400 snapshots for Power Spectra Density estimation.

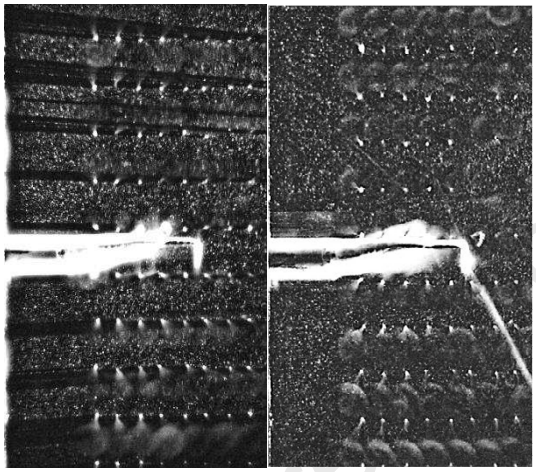

Figure 3 PIV images taken with an illumination sheet generated by a cylindrical rod lens alone (left) and with the cylindrical lens array (right).

The PIV velocity magnitude normal to the wire, or effective flow velocity, is: $|v| = \sqrt{{v_x}^2 + {v_y}^2}$, and was averaged as:

$$\overline{|v|} = \frac{1}{N}\sum_i |v|_i \,, \tag{1}$$

where N is the number of measurement snapshots. Here we have taken the average of the module for it is the module of the velocity normal to the wire that determines the heat transfer from the wire and therefore the hot wire anemometer measurement. The RMS fluctuation, on the other hand, is taken on the instantaneous velocity magnitude fluctuation, namely:

$$STD = \sqrt{\frac{1}{(N-1)}\sum_i \left(|v|_i - \overline{|v|}\right)^2} \,. \tag{2}$$

The error of the PIV measurements is therefore estimated as

$$ERR = \frac{STD}{\sqrt{N}} \tag{3}$$

where N is the number of measurements, which for the present work is 80. Assessing the uncertainties of individual PIV measurements is particularly challenging in flows through obstacles due to the abundance of light reflections. There is a number of different methods that can be used to estimate the uncertainty of PIV measurements obtained from typical images (Boomsma et al., 2016; Charonko and Vlachos, 2013; Sciacchitano et al., 2015, 2013). These methods have been

tested on high quality PIV image pairs and it is not clear whether they can be applied with the same confidence to images contaminated by multiple still elements. To get an upper bound of the errors, we set the flow so the maximum velocity in the test section reaches 0.15 m/s, in laminar regime, and locating the hot-wire probe at position P_2. The map of average velocity and the corresponding standard deviations calculated from the PIV measurements are shown in Figure 4. The STD indicates fluctuations from both, measurement noise and flow fluctuations. Flow fluctuations are only expected at the wake of the probe stem as a consequence of vortex shedding and they can be observed clearly in Figure 4. Measurement noise, on the other hand, is highest close to the wires that form the permeable medium and on the periphery of the measurement area. In the present work we focus on velocity values measured 1 mm upstream from the hot wire and at 10 mm upstream from the hot wire anemometer positions P_1, P_2, and P_3. For the 1 mm upstream the STD of the individual measurements is within 7 mm/s and for measurements at 10 mm upstream the STD is within 9 mm/s. These correspond to displacement errors of 0.49 pixels for measurements at 1 mm upstream and 0.63 pixels for the 10 mm upstream measurements. These values are slightly higher than typical uncertainty expected in PIV measurements (Sciacchitano et al., 2015) and most likely due to the presence of reflections in the PIV images.

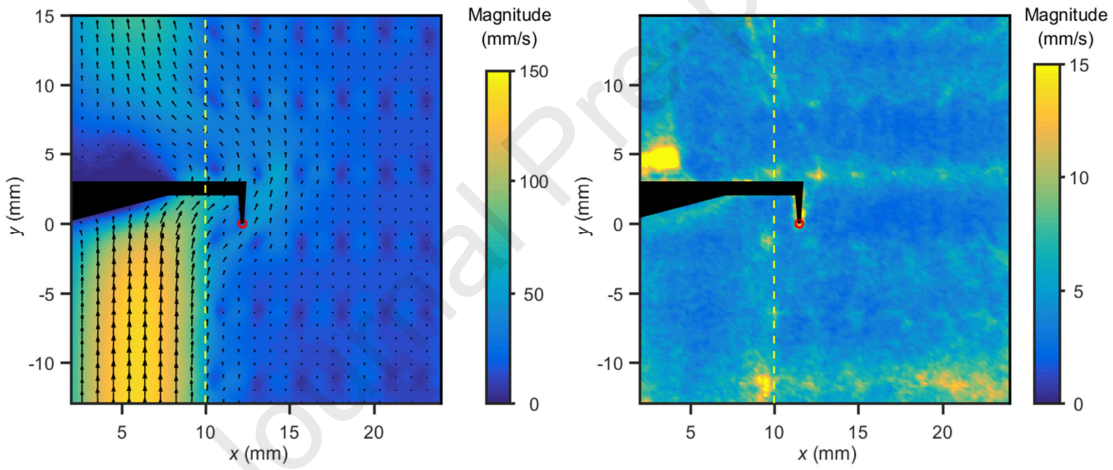

Figure 4. A typical averaged velocity field with the hot wire probe at position P_2, measured by PIV for steady laminar flow (left) and the velocity measurement STD field (right).

Ideally we would want to measure the velocity magnitude by PIV at the precise location of the hot wire. Alas, the optical access to this precise area is obstructed by the hot wire supports (See Figure 4). Therefore, a point located at (1.0 ±0.2) mm upstream the probe was chosen as the PIV local measurement for comparison with the HWA output. This selection is a compromise, being far enough from the perturbed region to get reliable PIV measurements, but at the same time sufficiently close to the probe to be representative of the HWA local flow velocity. The distance from the probe is approximately twice the local flow displacement between frames at the maximum velocity of interest.

Hot Wire Anemometry

In Figure 5 we show a photograph of the hot wire probe with the indication of the most relevant dimensions. The probe was specifically designed to pass through the gaps of the wire array entering from the side opposite to the incoming laser sheet. The diameter of the probe's stem is 4 mm and

the hot wire is supported by two tapered stainless steel wires (prongs) bent at 90 degrees. The diameter of the tips of the supporting prongs is (0.25±0.03) mm. The hot wire is spot welded to the prongs resulting in a total hot wire length of (1.9±0.1) mm. The wire used in the probe is a 15 µm Platinum with 10% Iridium unplated wire. This alloy presents better chemical stability than Tungsten while having a significantly higher tensile strength than pure Platinum at the cost of a lower temperature coefficient of resistivity. The wire diameter was chosen relatively large to reduce the sensitivity to particle dusting, that would lead to output drifts with time (Hewes, 2019), to increment the mechanical durability of the filament and to achieve a higher sensitivity (Ligęza, 2020). In addition, for a given heating power a thinner wire implies higher working temperatures, which would accelerate ageing of the wire and of the welding spots. A study of the effect of wire diameter on the sensor performance can be found in the work of Paweł Ligęza (Ligęza, 2020). A constant temperature bridge is used for the HWA system (details are reported in Osorio et al., 2010). The output from the HWA is acquired by a 12-bit data-acquisition board at a rate of 1000 samples per second. Each measurement consists of a 20-s sample.

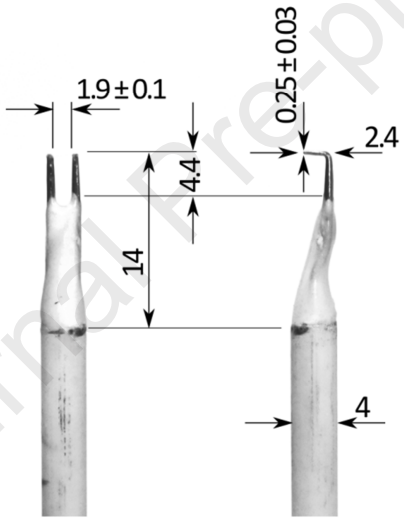

Figure 5 Hot wire probe used in the present study. The front view is on the left and the lateral view on the right (all dimensions are in milimeters).

The voltage signal from the HWA, when the probe is in stagnant air, presents fluctuations with a standard deviation value of 0.002 V and has a long term repeatability of the mean value within 0.001 V. With the anemometer operating at an overheat ratio of 1.4 this is equivalent to a noise of 0.004 m/s standard deviation and a repeatability within 0.002 m/s. This last was assessed by repeating measurements several times every 3 hours with the probe at position 3 on stagnated flow and a 1.4 overheat ratio.

There are some heat transfer issues that might affect the HWA measurements when used simultaneously with PIV. The presence of particles might change the heat-transfer rate of the HWA, introducing noise in the output signals. Also the laser might heat up the hot wire (Sciacchitano et al., 2015). To assess the magnitude of these sources of error, measurements were performed at 0.1 m/s

with and without seeding in the test section and with and without laser illumination. In both cases the observed differences were smaller than the measurement repeatability.

Results

HWA effect on the flow field

We have started by measuring the flow velocity field by means of PIV in the described test section with the HWA operating at an overheat ratio of 1.4. Measurements were taken with and without flow forcing, i.e. under natural convection and mixed convection respectively, and placing the probe in different positions within the channel, as described in the previous section.

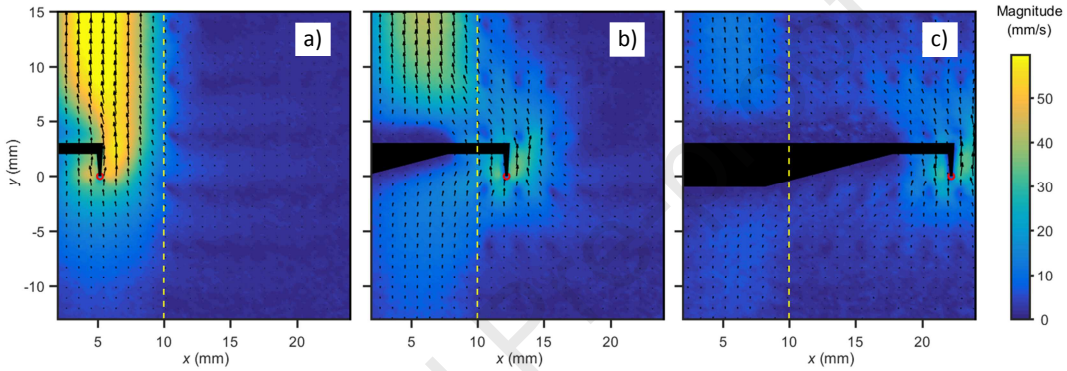

Figure 6. Flow average velocity fields in natural convection conditions, with the HWA operating at an overheat ratio of 1.4. a) With the hot wire probe at position P_1, b) at position P_2, and c) at position P_3.

Figure 6 shows the map of the average velocity field calculated from 80 PIV snapshots obtained in conditions of natural convection. Each graphic corresponds to a different position of the HWA, which was operating at an overheat ratio of 1.4. The natural convection plume induced by the hot wire can be seen downstream and around the probe. With the hot wire at position P_3 (see Figure 6 c), where the probe is deep in the permeable medium, the heating power of the wire induces localized flows in the neighborhood of the probe encompassing several representative volume elements of the permeable medium. As the hot wire gets closer to the free flow zone (Figure 6 b) the natural convection flow induced by the hot wire is diverted downstream to the free-flow zone, inducing an extended plume behind the probe. With the hot wire located in the free flow zone (Figure 6 a) the flow of the natural convection plume is significantly higher, reaching velocity values up to 60 mm/s. It is worth remarking that the presence of the hot wire not only perturbs the local velocity around the probe location, but it also produces a significant velocity increase in the free-flow layer downstream from the hot wire position.

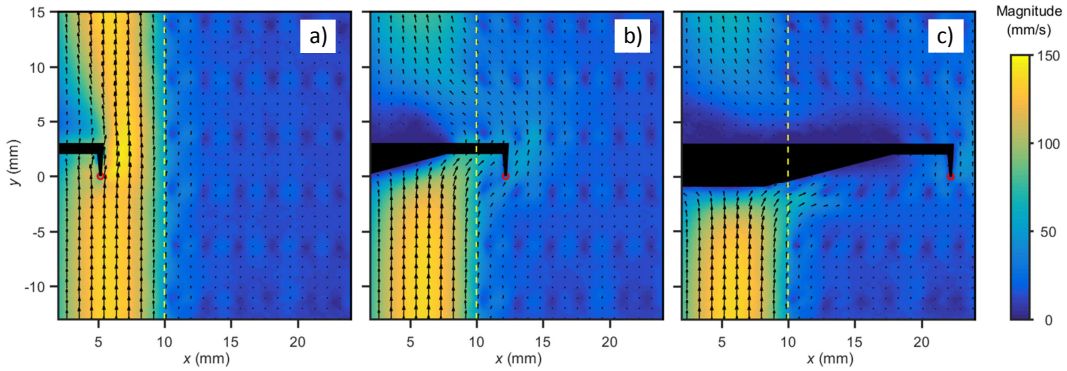

Figure 7. Average velocity fields with forced steady laminar flow, i.e. in mixed convection heat transfer, with the HWA operating at an overheat ratio of 1.4. a) With the hot wire probe at position P_1, b) at position P_2, and c) at position P_3.

Figure 7 shows the map of the average velocity field calculated from 80 PIV snapshots obtained in conditions of mixed convection. The forced flow is approximately the highest that could be reached in laminar flow regime in our experimental test section. The maximum velocity in the measurement region is approximately 0.15 m/s. The presence of the probe results in the diversion of the flow upstream, followed by a velocity increase as the flow circumvents the probe. The importance of these effects is determined by the shape of the stem and the length and diameter of the supports (Vagt, 1979).

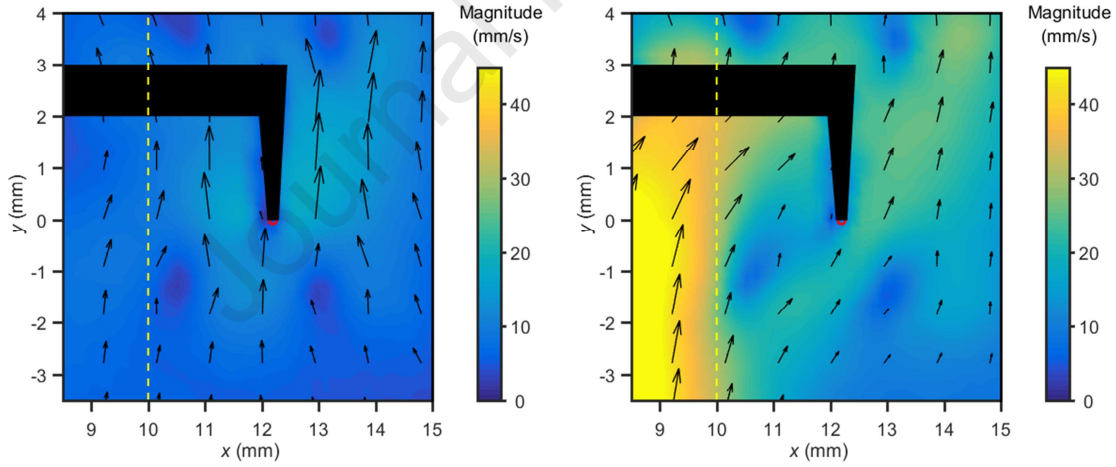

Figure 8. Detail of the flow field around the hot wire at position P_2 in natural convection (left) and mixed convection conditions (right). The HWA was operated at an overheat ratio of 1.4.

Figure 8 shows a detail of the velocity field around the probe at position P_2 in natural convection and mixed convection situations. In the natural convection situation (Figure 8, left), it can be observed that the affected zone extends beyond the nearest wires. Also the wires produce wakes that locally modify the flow and there is a channeling of the flow between the two permeable medium wires upstream from the probe. In contrast, for mixed convection conditions the flow is obstructed by the probe, in particular by the probe stem in the free flow region, which results in a diagonal flow reaching the hot wire. As a result there is a change in the relative distances between the wakes, the channeled flow, and the hot wire probe.

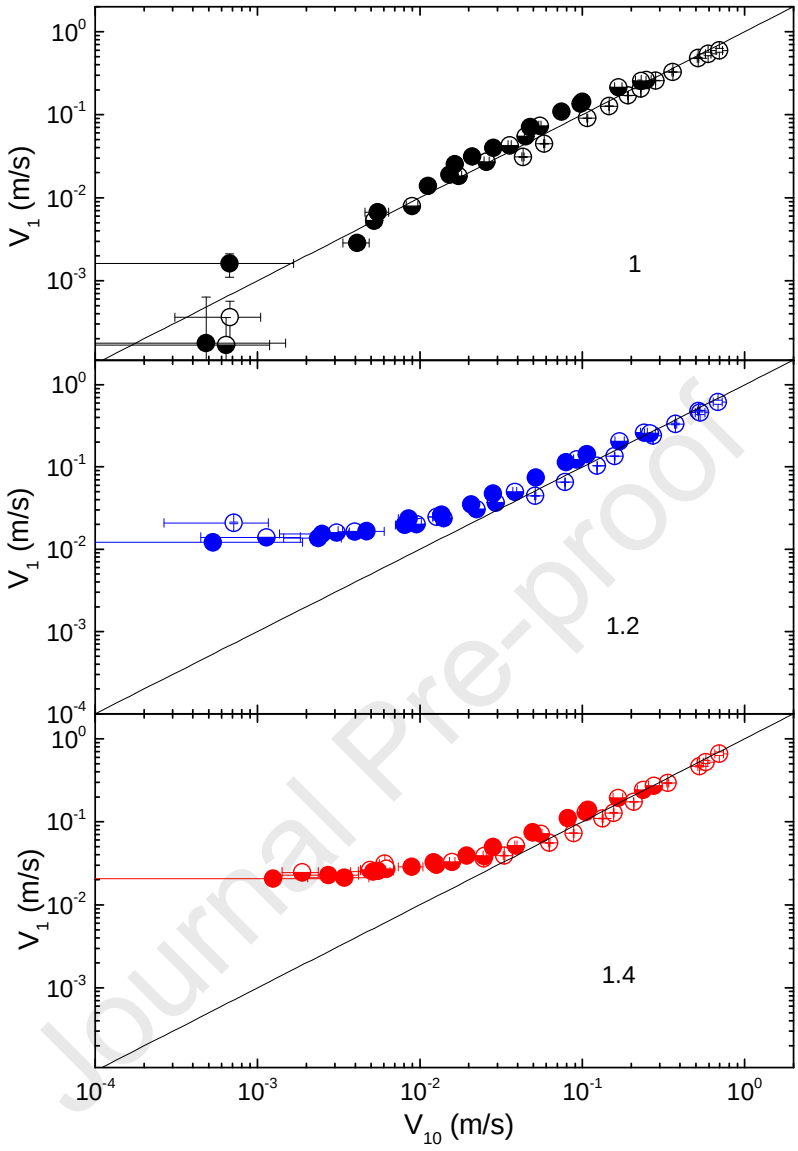

Figure 9. PIV velocity magnitude at 1 mm upstream from the hot wire as a function of the reference velocity measured at 10 mm upstream. The data are parametrized according to the overheat ratio: 1.4 (red), 1.2 (blue) and with no overheat (black). The symbols correspond to the position: free flow P_1 (empty), interface P_2 (half solid), and in the permeable region P_3 (solid).

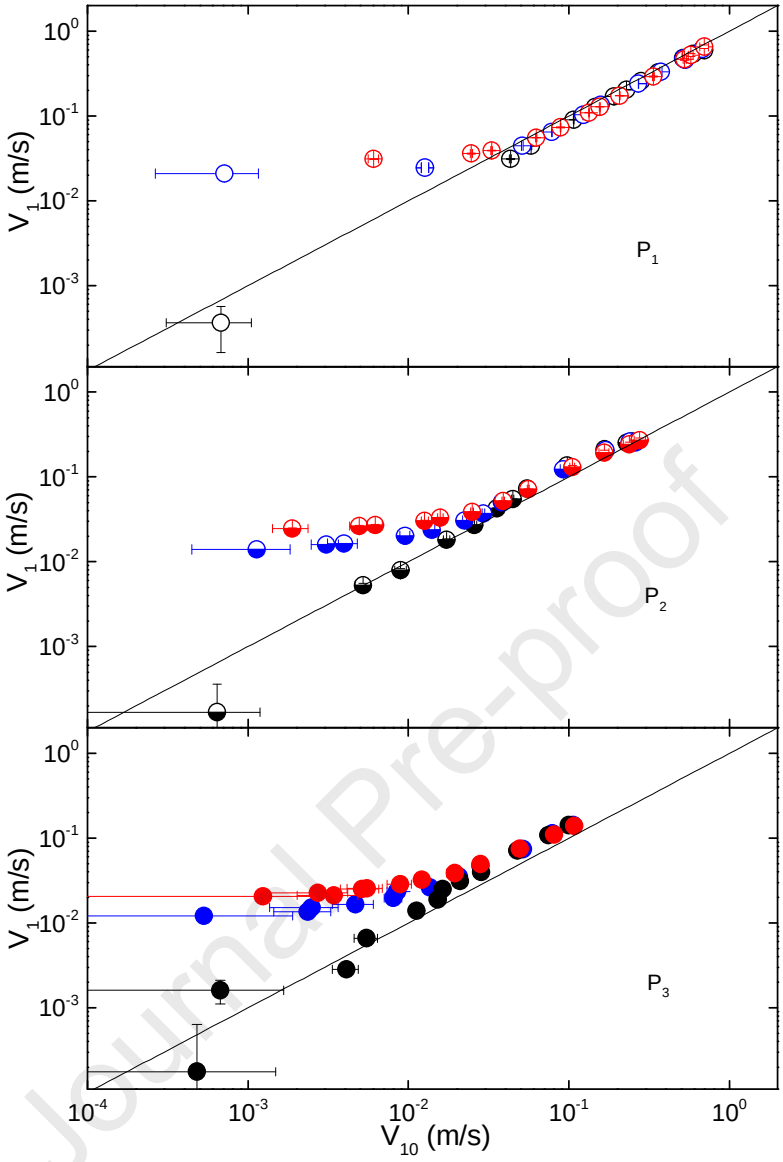

Figure 10. PIV velocity magnitude at 1 mm upstream from the hot wire as a function of the reference velocity measured at 10 mm upstream. The data are parametrized according to the position in the channel, namely, free flow P_1 (empty), interface P_2 (half solid), and in the permeable region P_3 (solid). The color of the symbols corresponds to the overheat ratio: 1.4 (red), 1.2 (blue) and with no overheat (black).

A series of PIV measurements, like those shown in Figure 7, were performed at different flow rates. The hot wire was placed at the three reference positions and operated at 0, 1.2 and 1.4 overheat ratios. These measurements were used to assess the degree of perturbation that the probe produces in the local velocity and quantify the HWA response in this type of permeable media. In order to make a quantitative assessment of these effects, we compare the velocity measured by PIV at a nearby upstream point, 1 mm from the probe tip in the flow direction, with the velocity at an upstream distance of 10 mm in the *y* direction. The latter will be considered to be the reference value that should have been measured without interference, whereas the former is the actual flow velocity reaching the hot wire. The results are presented in Figure 9 where the 1 mm-upstream velocity is plotted against the 10 mm-upstream velocity, for each HWA overheat. To better appreciate the differences of the probe intrusion depending on the presence or not of the permeable medium, Figure 10 shows the data gathered according to the probe position. The error

bars indicate the standard error of the velocity magnitude. In addition, Fig. 11 shows the velocity difference between the reference point at 10 mm (V_{10}) and 1 mm upstream from the hot wire (V_1) plotted against the latter. In all these graphics, the symbols correspond to the position: free flow P_1 (empty), interface P_2 (half solid), and in the permeable region P_3 (solid); whereas the color of the symbols corresponds to the overheat ratio: 1.4 (red), 1.2 (blue) and with no overheat (black).

Two regimes can be distinguished according to the observed relation between velocities V_{10} and V_1, namely, a constant offset (V_1 - V_{10}) for V_{10} < 0.03 m/s, and a more complex relation for V_{10} > 0.03 m/s. The threshold between both regimes is indicated in Fig. 11 with a dashed vertical line.

In the low velocity range (V_{10} < 0.03 m/s), the sole presence of the probe is barely intrusive, and the offset is negligible within the experimental error. In turn, when the HWA is active (blue and red symbols), the local velocity is higher than the 10 mm-upstream velocity due to induced natural convection, resulting in a velocity offset. The offset is (0.012 $\pm$ 0.003) m/s and (0.020 $\pm$ 0.003) m/s for 1.2 and 1.4 overheat ratio, respectively.

For V_{10} > 0.03 m/s, in the free flow position (empty symbols, position P_1) the mechanical intrusion of the probe becomes significant. Since V_1 is measured closer to the stagnation point, it tends to be lower than $V_{10.}$ The difference between V_{10} and V_1 increases with V_{10}, but the relative difference slowly decrease as V_{10} increases (15% and 10% at V_{10} 0.1 and 0.5 respectively). On the other hand, at position P_3, inside the permeable region (solid symbols), the velocity offset (V_{10} - V_1) increases as the V_{10} increases. This behavior holds up to the maximum velocity measured at position P_3, approximately 0.1 m/s. The differences between overheat ratios are within 0.01 m/s. At position P_2, near the border between the permeable and free flow zones, the relationship observed between V_1 and V_{10} is more complex. Between 0.03 and 0.1 m/s the offset (V_{10} - V_1) follows the same trend as in position P_3, increasing up to 0.045, 0.035 and 0.025 m/s for overheat ratios 1, 1.2 and 1.4, respectively, observed at V_{10} = 0.105 m/s. For higher velocities the offset drops, vanishing at approximately 0.3 m/s. The fact that V_1 is higher than V_{10} at P_1 and P_2 is explained by intrusive effect of the probe stem, which when the tip is at these positions blocks the free flow zone increasing the flow penetration into the permeable region. This can be observed in Figure 8 (right). Since the flow diversion is stronger the closer to the probe, velocity V_1 becomes higher than V_{10}.

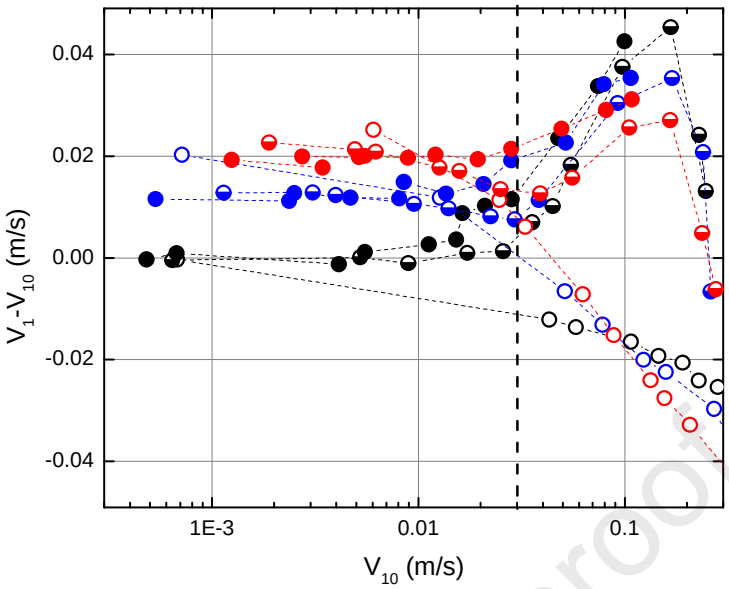

Figure 11 Velocity difference (offset) between the reference point at 10 mm (V_{10}) and 1 mm upstream from the hot wire (V_1). The symbols correspond to the position: free flow P_1 (empty), interface P_2 (half solid), and in the permeable region P_3 (solid). The color of the symbols corresponds to the overheat ratio: 1.4 (red), 1.2 (blue) and with no overheat (black).

Figure 12 depicts the 1 mm-upstream velocity at position P_3 (inside the permeable zone) under natural convection heat transfer, showing a linear dependence with the overheat ratio. This indicates that inside the permeable medium the Darcy drag is balanced by the buoyant forces, as in Elder's model for natural convection in porous media (Elder, 1967).

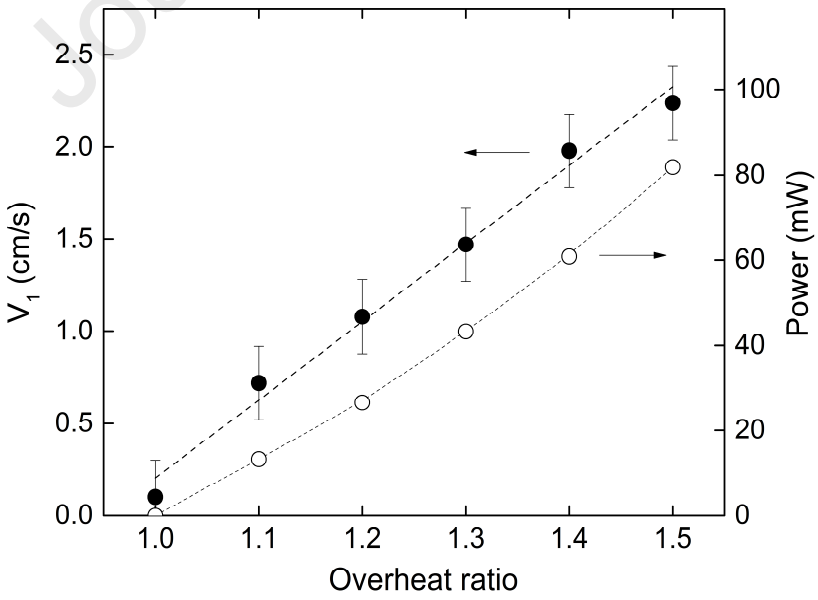

Figure 12. Dependence of the PIV velocity magnitude at 1 mm upstream from the probe, and the dissipated power in the hot wire, on the operating overheat ratio, under natural convection heat transfer.

Figure 13 shows the voltage output of the HWA as function of the 1 mm-upstream velocity measured by PIV, for overheat ratios of 1.2 and 1.4 respectively. The bars indicate the standard error of the measurements, which is larger at higher velocities due to higher fluctuations caused by shear instabilities. The largest fluctuations are observed at position P_2 starting at a local velocity of approximately 0.1 m/s. The response of the HWA is almost linear in most of the range shown in the figure. This linear behavior holds down to conditions dominated by natural convection, i.e. velocities lower than 0.03 m/s, except for the case of measurements with the hot wire at position P_1, which show lower HWA output values than those obtained with the hot wire at P_2 and P_3. It can be observed that the data obtained with the hot wire at the three different positions are very similar. For an overheat of 1.2 the HWA output corresponding to all three positions can be fit within experimental error by a single linear function in the range from 0.03 m/s to approximately 0.2 m/s. For the same velocity range but for an overheat ratio of 1.4 the data can be fit with a linear function with all residuals within 7% of the fitted HWA output values. It should also be noted that the dispersion of the measurements cannot be explained entirely on account of PIV or HWA measurement errors. In fact, there is another source of variation most likely originated by fluctuations in direction of jets from the free flow to the permeable medium (see Figure 8, right). The interaction of these jets with the small scale mixed convection flow around the hot wire is quite complex, and its detailed characterization exceeds the possibilities of the present experimental setup.

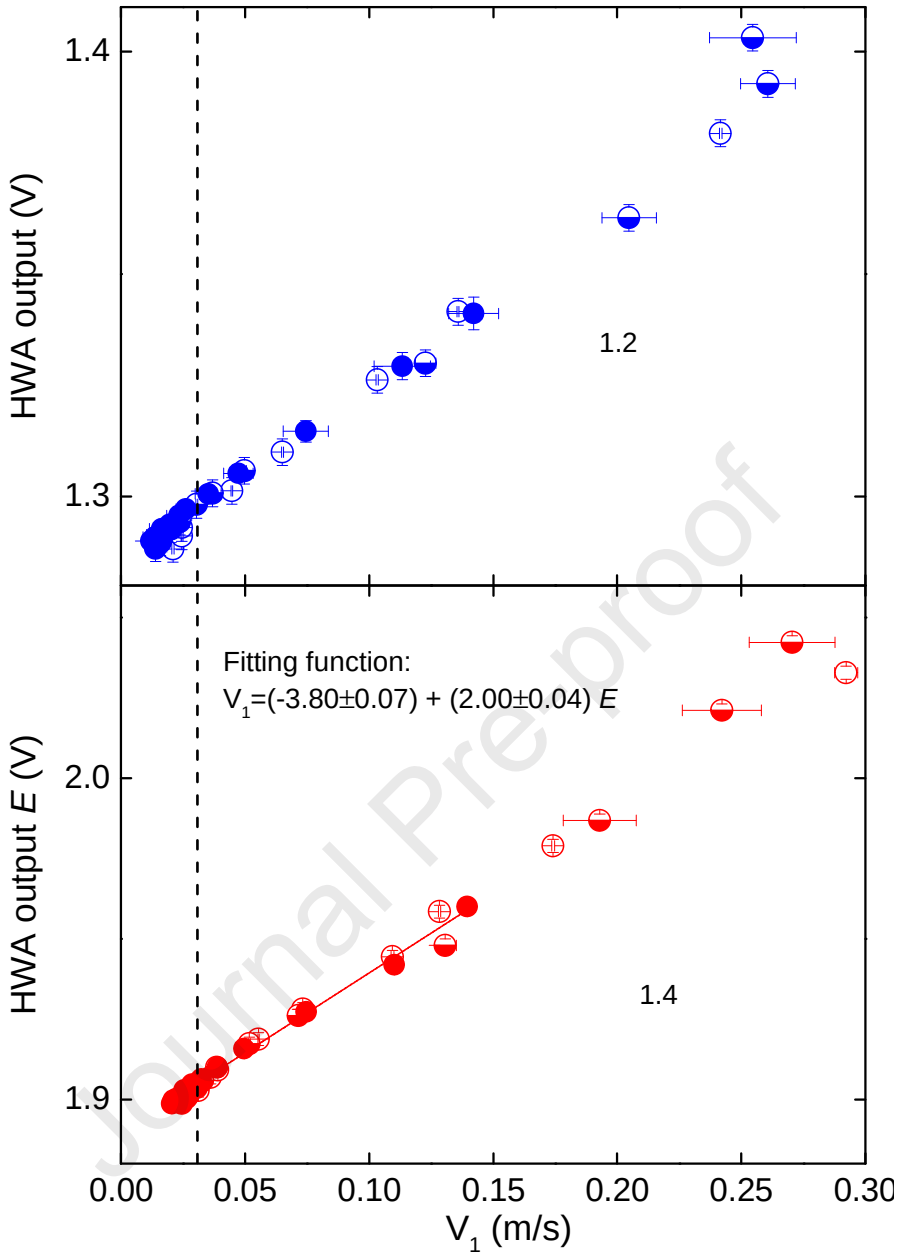

Figure 13. Variation of the voltage output of the HWA with the 1 mm-upstream velocity measured with PIV, placing the probe at positions P_1 (empty circles), P_2 (half-empty circles), P_3 (solid circles). Overheat ratio= 1.2 (blue) and 1.4 (red). The fitting function, that is used as anemometer calibration, corresponds to measurements at P_3 with an overheat ratio of 1.4.

Thermal losses from the hot wire to the permeable structure

Figure 14 shows the profile of the HWA output for different traverse positions. Measurements are performed with an overheat ratio of 1.4. The dashed lines in the graphic indicate the positions of the obstruction wires. It can be observed that the HWA reading peaks at these positions, which corresponds to velocity variations of about 3 mm/s. These variations cannot be ascribed to self-induced natural convection, because if so the peaks would be located in the gap between wires. This

effect is probably due to enhanced heat transfer from the HWA to the structure wires, in accord with other reports of HWA near solid walls (Ikeya et al., 2017).

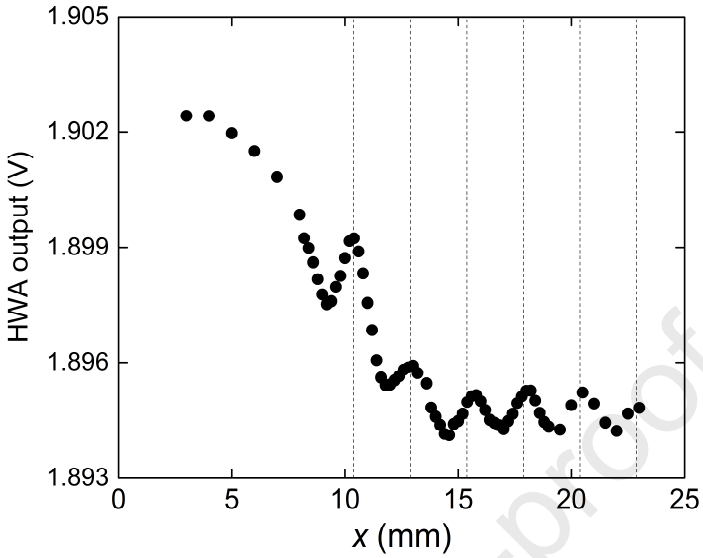

Figure 14. Transversal profile of the HWA output signal under natural convection conditions and operating with an overheat ratio of 1.4.

Thermal losses from the hot wire to its supports

Another important issue is the thermal losses by axial conduction from the wire to the supports (Freymuth, 1979), which becomes important at lower air velocities as the convective heat transfer diminishes. To estimate the importance of this critical issue, we measured the voltage drop and the current through the hot wire, and calculated the resistance of the hot wire and the heating power for each overheat ratio. The measurements were performed under natural convection at position P_3. The current was measured with a (47±1) mΩ shunt resistor in series with the hot wire probe. The corresponding heating power at each overheat ratio is shown in Figure 12. The heat losses from the hot wire to the supports have been be estimated by assuming conduction through the wire in one dimension with uniform convective heat transfer and Joule heating (Lord, 1974). Knowing the temperature dependence of the wire electrical resistivity, the heat transfer coefficient was adjusted iteratively until the calculated wire total resistance matched the measured value. The wire resistance at ambient temperature (22.1°C) is (2.8 ± 0.1) Ω. The relatively large uncertainty comes from the contact resistance between the sensor wire and the supports and the resistance of the supports themselves (Ligęza, 2000). The average temperature of the wire for overheat ratio 1.4 is (362 ± 30) °C and the resulting calculated losses to the supports is approximately 16 mW. The calculated losses account for 25% of the total 62 mW dissipated by the hot wire according to the experimental measurements. The estimated Nusselt number is 0.62. In turn, Morgan's (1975) correlation for long cylinders gives a Nusselt number of approximately 0.4. The higher value estimated for the hot wire in the probe is due to the small aspect ratio of the wire and the flow interference produced by the supports. Further discussion of the effect of the wire length on natural convection from small wires can be found in the work of Morgan (1975).

Dynamic response of the hot wire

A useful application of HWA is the characterization of flow stability, in particular to measure flow oscillations in low speed flows. In our test section, the position where fluctuations are largest is at the boundary between the permeable medium and the free flow. Figure 15 shows the map of the relative standard deviation (RSD) of the velocity magnitude for a forced flow with a maximum velocity of 0.43m/s. The RSD is calculated as the RMS divided by the local time average. It can be seen that the maximum RSD values are found in the region of P_2. At this position, Kelvin- Helmholtz instabilities produce periodic coherent waves that propagate along the channel (Silin et al, 2011; Boroni et al, 2015). In these conditions the local velocity, measured at 1mm upstream from P_2 has a time mean velocity magnitude of (0.131 ± 0.012) m/s and a fluctuation STD of (0.039 ± 0.006) m/s.

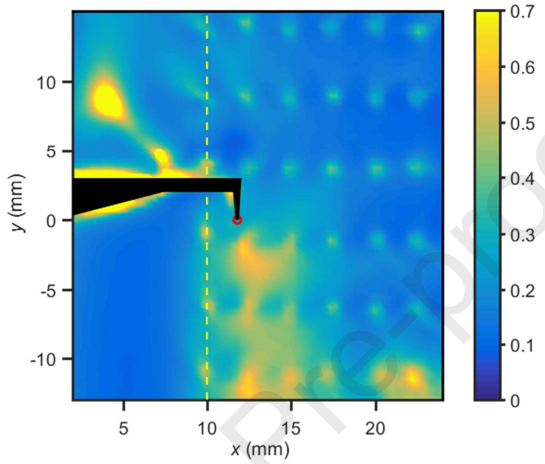

Figure 15 Relative Standard Deviation map for conditions of unstable flow in the test section and with the hot wire probe at position P_2. The maximum velocity in the test section is 0.43m/s.

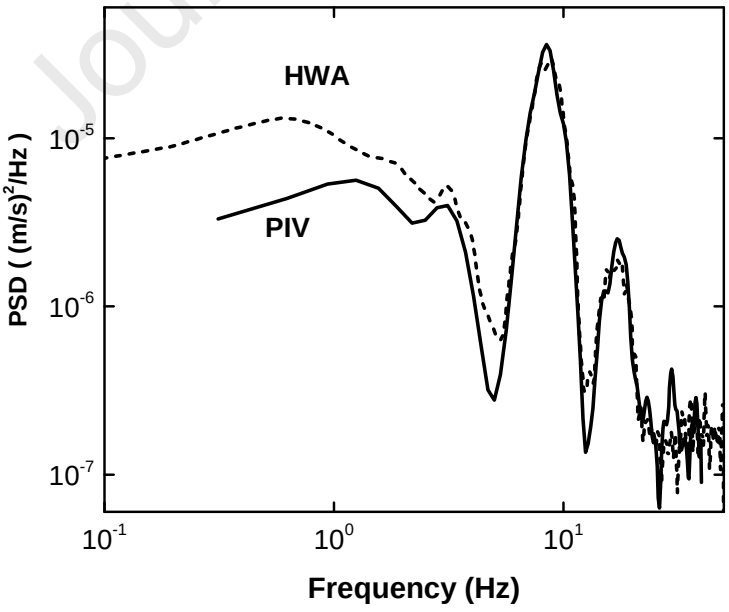

Figure 16. PSD obtained from PIV velocity measurements 1 mm upstream from the hot wire and from the corresponding HWA signal.

To study the dynamic response of the HWA, the time resolved PIV measurements were synchronized with the HWA measurements at position P_2. The PIV measurements were taken at a rate of 80 velocity snapshots per second during 5 s, while the HWA measurements were acquired at 1000 samples per second during 20 s. The latter were converted to velocity units by means of the calibration curve shown in Figure 13. The power spectra of the PIV velocity magnitude at 1 mm upstream from the hot wire and the HWA output are compared in Figure 16. Two clear peaks are identified at frequencies of approximately 8.5 and 17 Hz. The second is probably a harmonic of the first dominating frequency. The good agreement between both spectra indicates that the HWA response is faster than the velocity fluctuations, which validates the use of HWA for the study of this type of instabilities up to at least 20 Hz. This result is not trivial because the Peclet number of the wire is very low, 0.014, indicating that the heat transfer from the wire is dominated by conduction through the air rather than convection, and therefore the thermal response of the hot wire should be significantly deteriorated. However, as can be seen in the graphic, this effect does not hinder the measurements within the range of frequencies that occur in the present experimental setup. The relative minima are higher for the HWA due to the higher noise of its signal. At low frequencies the differences are due to the different sampling times.

Discussion

The PIV velocity field shows clearly that the natural convection flow induced by the hot wire extends over several obstruction elements (see Figure 6). Yet, a closer look around the hot wire reveals that the velocity is also affected by the obstruction elements of the permeable medium (see Figure 8). The self-induced flow velocity is lower inside the obstructed rather than in the unobstructed flow.

For the thin wires used in hot wire anemometry and at very low velocities, like those encountered inside the obstruction, the heat transfer close to the wire is dominated by conduction, whereas convection becomes more relevant at larger distances from the wire. This is called the Langmuir stagnant film hypothesis (Mahony, 1957). Following the model of Seiichi and Takuro (Seiichi and Takuro, 1975) for natural convection from fine wires, the transition between the conductive and the convective regimes occurs at a radial distance r_c given by:

$$\frac{r_c}{d} = Pe^{-1} = (Re\ Pr)^{-1} = \alpha/Vd \qquad (4)$$

where d is the wire diameter, V is the characteristic velocity and α the thermal diffusivity. The magnitude r_c can be understood as the distance at which conductive and the convective heat transfer are comparable, for smaller distances conduction is the dominating heat transfer mechanism while for larger distances the heat transfer will be dominated by convection. For overheat ratio 1.4 and in natural convection conditions, the induced velocity measured 1 mm upstream from the wire is approximately 0.02 m/s and therefore, according to Eq. (4), r_c becomes approximately 1 mm. It is expected that any solid with a thermal conductivity higher than the fluid, located at or closer than a distance r_c from the hot wire, will increase the conductive heat transfer from the hot wire. In our case the distance between the HWA and the closest row of wires (see Figure 1) is similar to r_c, which is consistent with the interpretation that the local maxima in Figure

14 are caused by conduction heat transfer to the wires. The value of r_c for this operating condition is also comparable with the length of the hot wire, therefore conduction through the air in the direction parallel to the hot wire to the prongs is also significant. As a consequence heat transfer from the hot wire becomes a conjugate heat transfer problem and the hot wire cannot be assumed to be slender from the thermal point of view. Alas, this cannot be prevented by using a thinner wire, because r_c does not depend on d, it can only be prevented by using a longer wire, at the cost of reduced spatial resolution and perhaps an increased intrusivity. A discussion on this topic is presented by Mahony (1957), who studied the problem of natural convection in long horizontal fine wires. He showed that at very low local Grashof numbers the large thickness of the conductivity layer requires very high length-to-diameter ratios in order to achieve a line-source type of behavior. Hence, typical HWA probes with length-to-diameter ratios in the order of 200 operated at very low velocities cannot be considered slender. This thick conduction layer indicated by a relatively large value of r_c is also compatible with the findings of Kjellstrom and Hedberg (1970). In their work they notice that at low wire Reynolds numbers the measurement is significantly affected by the wire parallel component of the velocity. Naturally, if there is an increase of external velocity it will be reflected in a reduction of r_c and consequently an improvement of the HWA performance.

The dynamic response of the HWA will be determined by the time it takes for a change in the flow velocity to affect the heat removal from the hot wire. Since the time response of the feedback electronic circuitry that controls the temperature of the hot wire is several orders of magnitude faster than the involved thermal lags, the heat capacity of the wire can be neglected. From dimensional considerations the thermal characteristic time of the conduction layer, i.e. the thermal near field, should be:

$$\tau \sim \frac{{r_c}^2}{\alpha} \tag{5}$$

For the self-induced natural convection flow at 1.4 overheat, Eq. (5) gives $\tau \sim 0.05\, s$. The corresponding cut-off frequency is about 20 Hz. Nevertheless, since Eqs. (4) and (5) ensure that the response time diminishes with the square of the flow velocity, the HWA will rapidly improve the dynamic performance with increasing flow velocities. This order of magnitude estimation is consistent with the experimental results presented in Figure 16.

Conclusions

Particle Image Velocimetry was applied in a test section partially occupied by a permeable obstruction to measure the flow field around an operating Hot Wire Anemometer. The test section was placed vertically with an upward forced flow, in the same direction as the natural convection plume induced by the HWA. The setup was chosen because it is better suited for the application of HWA to the measurement of low velocity flows.

When measuring with the hot wire under self-induced natural convection heat transfer, the region showing an increased velocity due to the natural convection flow extends upstream (downwards) and also laterally over several representative volume elements of the permeable medium, whereas downstream (upwards) it extends well beyond the field of view of the PIV setup. We have also

observed that when the hot wire is placed inside the obstruction but close to the free-flow border, the thermal plume extends even into the free flow zone. On the other hand for low forced flow velocities the HWA probe introduces a significant blockage, although generally this phenomenon is expected to depend on the probe design and on how it is inserted in the test section.

As expected, the natural convection induced by the hot wire contributes to increasing the flow velocity around the hot wire itself, leading to overestimations of the local unperturbed velocity. When the HWA is operated inside the permeable obstruction in natural convection conditions, the induced local velocity measured 1 mm upstream from the wire increases linearly with the overheat ratio. This behavior differs from the dependence observed in free flows (Seiichi and Takuro, 1975), but is consistent with previous analysis of natural convection in porous media by Elder (Elder, 1967).

We have compared the output signal of the HWA with the local velocity V1 measured by PIV at 1 mm upstream from the hot wire. Operating with overheat ratio 1.2, the HWA output signal correlates linearly with V1, ranging from 0.03 to 0.2 m/s. This behavior holds in the permeable obstruction as well as in the free flow. A similar linear dependence is also observed operating the HWA with overheat ratio 1.4, although in this case the data are more scattered. The latter cannot be ascribed solely to PIV and HWA measurement errors, but it might be caused by the interaction with small scale flow features occurring in the permeable region (see Figure 8).

All in all, the flow produced by natural convection self-induced by the HWA probe can be regarded as an offset respect to the flow reference velocity, which in our case was measured 10 mm upstream from the hot wire position. Figure 11 shows the dependence of such offset on both the reference velocity and the overheat ratio. An interesting conclusion is that for internal flows, the low speed offset produced by the hot wire depends on the measurement section geometry, even in the free flow region. The characterization of this effect is beyond the scope of the present study, but it is an issue that should be considered when using HWA for internal flows al low speeds.

When traversing the hot wire at 1-mm distance from a row of wires forming the permeable obstruction, in natural convection conditions, the HWA output increases at the positions closer to the wires. This phenomenon is presumably related to conductive heat transfer to the obstacles, a phenomenon well studied in boundary layer measurements. This hypothesis is also compatible with the estimated 1-mm size of the conduction-dominated region around the hot wire, which is even larger for smaller overheat ratios. In the present study the importance of this phenomenon is minor compared with other error sources, but in other applications the relevance of this phenomenon will depend on the geometry and material of the obstructions under study (Ikeya, 2017). Furthermore the conduction-dominated region is similar in size to the length of the wire, which suggests that at very low flow velocities the wire cannot be regarded as slender from a thermal point of view, as already suggested by previous works (Mahony, 1957).

Finally, the dynamic response of the HWA was verified in a flow condition where large flow velocity oscillations are present, by comparing the spectra of both measurement techniques, i.e., HWA and PIV. The HWA showed a satisfactory response up to at least 20 Hz for a local mean velocity of (0.131 ± 0.012) m/s.

Acknowledgement: This project was partially supported by MINCYT through the project PICT-2016-0441 and by Universidad Nacional de Cuyo through the project 06/C595 . The authors wish to thank Diego Dalponte, Gustavo Sepúlveda and Ernesto Scerbo for their help with the construction of the experimental device.

References

Ali, S.A.S., Azarpeyvand, M. and da Silva, C.R.I., 2018. Trailing-edge flow and noise control using porous treatments. Journal of Fluid Mechanics, 850, pp.83-119.

Bodling, A. and Sharma, A., 2018. Numerical investigation of low-noise airfoils inspired by the down coat of owls. Bioinspiration & biomimetics, 14(1), p.016013.

Boomsma, A., Bhattacharya, S., Troolin, D., Pothos, S., Vlachos, P., 2016. A comparative experimental evaluation of uncertainty estimation methods for two-component PIV. Meas. Sci. Technol. 27, 094006. https://doi.org/10.1088/0957-0233/27/9/094006

Boroni, G., Silin, N., Dalponte, D., Dottori, J. and Clausse, A., 2015. Lattice-Boltzmann modeling of unstable flows amid arrays of wires. Computers & Fluids, 120, pp.37-45.

Breugem, W.P., Boersma, B.J. and Uittenbogaard, R.E., 2006. The influence of wall permeability on turbulent channel flow. *Journal of Fluid Mechanics*, *562*, pp.35-72.

Bruun, H.H., 1996. Hot-wire anemometry: principles and signal analysis. Oxford University Press.

Charonko, J.J., Vlachos, P.P., 2013. Estimation of uncertainty bounds for individual particle image velocimetry measurements from cross-correlation peak ratio. Meas. Sci. Technol. 24, 065301. https://doi.org/10.1088/0957-0233/24/6/065301

Christman, P.J., Podzimek, J., 1981. Hot-wire anemometer behaviour in low velocity air flow. J. Phys. E: Sci. Instrum. 14, 46–51. https://doi.org/10.1088/0022-3735/14/1/013

Clausse, A., Silin, N. and Boroni, G., 2019. A multiscale method for producing homogenized drag laws of a permeable medium by conflating experimental data with Lattice-Boltzmann simulations. International Journal of Numerical Methods for Heat & Fluid Flow 29, 4394-4407.

Clark, I., Alexander, W.N. and Devenport, W.J., 2017. Bio-inspired finlets for the reduction of marine rotor noise. In 23rd AIAA/CEAS Aeroacoustics Conference (p. 3867).

Collis, D.C., Williams, M.J., 1959. Two-dimensional convection from heated wires at low Reynolds numbers. Journal of Fluid Mechanics 6, 357–384. https://doi.org/10.1017/S0022112059000696

Drew, B., Charonko, J., Vlachos, P.P., 2015. Qi - Quantitative Imaging (PIV and more) [WWW Document]. SourceForge. URL https://sourceforge.net/projects/qi-tools/ (accessed 8.6.19).

Eckstein, A., Vlachos, P.P., 2009. Digital particle image velocimetry (DPIV) robust phase correlation. Meas. Sci. Technol. 20, 055401. https://doi.org/10.1088/0957-0233/20/5/055401

Elder, J.W., 1967. Steady free convection in a porous medium heated from below. Journal of Fluid Mechanics 27, 29–48. https://doi.org/10.1017/S0022112067000023

Fand, R.M., Steinberger, T.E., Cheng, P., 1986. Natural convection heat transfer from a horizontal cylinder embedded in a porous medium. International Journal of Heat and Mass Transfer 29, 119–133. https://doi.org/10.1016/0017-9310(86)90040-2

Farsad, S., Ardekani, M.A., Farhani, F., 2019. Experimental investigation of aerodynamic effects of probe on heat transfer from hot-wire sensors at vertical and horizontal orientations. Flow Measurement and Instrumentation 70, 101642. https://doi.org/10.1016/j.flowmeasinst.2019.101642

Finnigan, J.J., Shaw, R.H. and Patton, E.G., 2009. Turbulence structure above a vegetation canopy. Journal of Fluid Mechanics, 637, 387-424.

Freymuth P., 1979. Engineering estimation of heat conduction loss inconstant temperature thermal sensors. TSI Quart.53–8.

Gayev, Y.A., Hunt, J.C.R. (Eds.), 2007. Flow and Transport Processes with Complex Obstructions: Applications to Cities, Vegetative Canopies and Industry, Nato Science Series II: Springer Netherlands. https://doi.org/10.1007/978-1-4020-5385-6

Ghisalberti, M., 2009. Obstructed shear flows: similarities across systems and scales. Journal of Fluid Mechanics, 641, 51-61.

Harshani, H.M.D., Galindo-Torres, S.A., Scheuermann, A. and Muhlhaus, H.B., 2017. Experimental study of porous media flow using hydro-gel beads and LED based PIV. Measurement Science and Technology, 28(1), p. 015902.

Hewes, A., Medvescek, J., Mydlarski, L.B. and Baliga, B.R.R., 2019. Drift compensation in thermal anemometry. Measurement Science and Technology, *in press.*

Ho, H.Q., Asai, M., 2018. Experimental study on the stability of laminar flow in a channel with streamwise and oblique riblets. Physics of Fluids 30, 024106. https://doi.org/10.1063/1.5009039

Ikeya, Y., Örlü, R., Fukagata, K., Alfredsson, P.H., 2017. Towards a theoretical model of heat transfer for hot-wire anemometry close to solid walls. International Journal of Heat and Fluid Flow 68, 248–256. https://doi.org/10.1016/j.ijheatfluidflow.2017.09.002

Ledda, P.G., Siconolfi, L., Viola, F., Gallaire, F. and Camarri, S., 2018. Suppression of von Kármán vortex streets past porous rectangular cylinders. Physical Review Fluids, 3(10), p.103901.

Ligęza, P., 2020. Static and dynamic parameters of hot-wire sensors in a wide range of filament diameters as a criterion for optimal sensor selection in measurement process. Measurement 151, 107177. https://doi.org/10.1016/j.measurement.2019.107177

Ligęza, P., 2000. Four-point non-bridge constant-temperature anemometer circuit. Experiments in Fluids 29, 505–507. https://doi.org/10.1007/PL00007121

Ligrani, P.M., Bradshaw, P., 1987. Spatial resolution and measurement of turbulence in the viscous sublayer using subminiature hot-wire probes. Experiments in Fluids 5, 407–417. https://doi.org/10.1007/BF00264405

Lord, R.G., 1974. Hot-wire probe end-loss corrections in low density flows. J. Phys. E: Sci. Instrum. 7, 56–60. https://doi.org/10.1088/0022-3735/7/1/015

Mahajan, R.L., Mahajan, R.L., 1980. Hot-wire anemometer calibration in pressurized nitrogen at low velocities. J. Phys. E: Sci. Instrum. 13, 1110–1118. https://doi.org/10.1088/0022-3735/13/10/016

Mahony, J.J., 1957. Heat Transfer at Small Grashof Numbers. Proceedings of the Royal Society of London. Series A, Mathematical and Physical Sciences 238, 412–423.

Morgan, V.T., 1975. The overall convective heat transfer from smooth circular cylinders. Advances in heat transfer 11, 199-264.

Osorio, O.D., Silin, N. and Converti, J., 2010. Fabrication of hot-wire probes and electronics for constant temperature anemometers. Latin American applied research, 40(3), 233.

Özahi, E., Çarpınlıoğlu, M.Ö., Gündoğdu, M.Y., 2010. Simple methods for low speed calibration of hot-wire anemometers. Flow Measurement and Instrumentation 21, 166–170. https://doi.org/10.1016/j.flowmeasinst.2010.02.004

Rosti, M.E., Brandt, L. and Pinelli, A., 2018. Turbulent channel flow over an anisotropic porous wall–drag increase and reduction. Journal of Fluid Mechanics, *842*, pp.381-394.

Sciacchitano, A., Neal, D.R., Smith, B.L., Warner, S.O., Vlachos, P.P., Wieneke, B., Scarano, F., 2015. Collaborative framework for PIV uncertainty quantification: comparative assessment of methods. Meas. Sci. Technol. 26, 074004. https://doi.org/10.1088/0957-0233/26/7/074004

Seiichi, N., Takuro, O., 1975. Heat transfer from a horizontal circular wire at small Reynolds and Grashof numbers—II: Mixed convection. International Journal of Heat and Mass Transfer 18, 397–413. https://doi.org/10.1016/0017-9310(75)90029-0

Silin, N., Converti, J., Dalponte, D. and Clausse, A., 2011. Flow instabilities between two parallel planes semi-obstructed by an easily penetrable porous medium. Journal of Fluid Mechanics, 689, 417-433.

Silin, N., Tarrio, J., Guozden, T., 2017. An experimental study of the aerodynamic dispersion of loose aggregates in an accelerating flow. Powder Technology 318, 151–161. https://doi.org/10.1016/j.powtec.2017.05.043

Vagt, J.-D., 1979. Hot-wire probes in low speed flow. Progress in Aerospace Sciences 18, 271–323. https://doi.org/10.1016/0376-0421(77)90010-0

Yue, Z. and Malmström, T.G., 1998. A simple method for low-speed hot-wire anemometer calibration. Measurement Science and Technology, 9(9), 1506.

Zanoun, E.-S., Durst, F., Shi, J.-M., 2009. The physics of heat transfer from hot wires in the proximity of walls of different materials. International Journal of Heat and Mass Transfer 52, 3693–3705. https://doi.org/10.1016/j.ijheatmasstransfer.2009.01.048

Highlights:

- Hot Wire Anemometers generate a natural convection plume
- The natural convection flow field was measured by Particle Image Velocimetry
- Natural convection introduces a velocity offset that is reflected in the HWA measurement
- The natural convection plume is modified by the presence of flow obstructions

AUTHORSHIP STATEMENT

Manuscript title: **Experimental Assessment on the Performance of Hot Wire Anemometry in and around a Permeable Medium by comparison with Particle Image Velocimetry**

All persons who meet authorship criteria are listed as authors, and all authors certify that they have participated sufficiently in the work to take public responsibility for the content, including participation in the concept, design, analysis, writing, or revision of the manuscript. Furthermore, each author certifies that this material or similar material has not been and will not be submitted to or published in any other publication before its appearance in the journal "Flow Measurement and Instrumentation"

Acknowledgements: All persons who have made substantial contributions to the work reported in the manuscript (e.g., technical help, writing and editing assistance, general support), but who do not meet the criteria for authorship, are named in the Acknowledgements and have given us their written permission to be named.

This statement is signed by all the authors.

Nicolás Silin 25/AUG/2020

Diego Cuscueta 25/AUG/2020

Alejandro Clausse 25/AUG/2020

Declaration of interests

☒ The authors declare that they have no known competing financial interests or personal relationships that could have appeared to influence the work reported in this paper.

☐The authors declare the following financial interests/personal relationships which may be considered as potential competing interests: